PACS numbers: 42.55.Px; 42.60.Lh
DOI: 10.1070/QE2002v032n03ABEH002176

Effect of amplified luminescence on the lasing threshold of long-wavelength injection lasers

L.I.Burov, I.N.Varaksa, S.V.Voitikov, M.I.Kramar, A.G.Ryabtsev, G.I.Ryabtsev

***Abstract*. By solving radiation-transfer equations, we studied the effect of amplified luminescence on the lasing threshold of long-wavelength injection InGaAsP/InP lasers with bulk and quantum-well active layers emitting in the range from 1.3 to 1.55 μm. The amplified luminescence trapped in the resonator of a stripe laser can result in an increase in the threshold current density by a factor of two and more. It is shown that the effect of amplified luminescence on the temperature dependence of the threshold current is most pronounced in longer-wavelength lasers and, all other factors being the same, in lasers with a quantum-well active layer.**

Keywords: *injection laser, amplified luminescence, lasing threshold.*

The amplification of luminescence in the active layer of a semiconductor laser results in an increase in the threshold current density J_{th} and a decrease in the output power [1 – 4]. The amplified luminescence flux density in the resonator of an injection laser (IL) can become sufficient not only for a noticeable decrease in the spectral gain k_ν but also for bleaching of the passive regions of a heterostructure [5, 6]. The recombination rate R_{lum} induced by amplified luminescence depends on the material of the IL active layer, the resonator parameters, the pump energy and temperature [4, 7]. All other factors being the same, the rate R_{lum} is greater for the InGaAsP/InP heterostructures emitting in the long-wavelength region between 1.3 and 1.55 μm than for aluminium – gallium arsenide ILs emitting in the near IR region [7, 8].

Analysis of the temperature dependences $R_{lum}(T)$ and $J_{th}(T)$ [7, 8] showed that amplified luminescence, along with Auger recombination, the temperature broadening of the gain spectrum, leakage currents through potential barriers of the heterostructure, etc. [9 – 11], is one of the factors determining the temperature dependence of the lasing threshold of long-wavelength injection lasers. The recombination rate R_{lum} can be calculated from the equation for the spontaneous radiation balance [7]. However, this approach not always allows one to take into account the dependence of R_{lum} on the geometrical parameters of the IL active layer.

In this paper, we calculated the recombination rate R_{lum} by solving radiation-transfer equations for amplified luminescence, which allow us to simulate correctly the development of radiation in the IL resonator. We used the results of calculations for estimating the effect of amplified luminescence on the temperature dependence of the lasing threshold of long-wavelength ILs. The numerical data were obtained for InGaAsP/InP lasers with bulk and quantum-well active layers and stripe contact.

Using the concepts developed for solid-state lasers [12], we can write the system of self-consistent equations describing the transfer of amplified luminescence in the active layer of long-wavelength ILs in the form

$$\frac{1}{b(z)}\frac{\mathrm{d}S_\nu^{\pm}(z)}{\mathrm{d}z} = \left[\frac{k_\nu(z)}{1+\varepsilon\tilde{S}(z)} - \rho\right]S_\nu^{\pm}(z) + ar_{lum}(z), \qquad (1)$$

$$\frac{J}{ed} = An + Bn^2 + Cn^3 + R_{lum}(z), \qquad (2)$$

where $k_\nu(z)$ is the spectral gain at frequency ν at the point z of the resonator axis; $S_\nu^+(z)$ and $S_\nu^-(z)$ are the spectral densities of amplified luminescence fluxes counterpropagating along the resonator axis z; $\tilde{S}(z) = \int[S_\nu^+(z) + S_\nu^-(z)]\mathrm{d}\nu$ is the amplified luminescence flux density at the point z of the resonator axis integrated over the frequency and propagation directions; ρ is the coefficient of internal optical losses; e is the electron charge;

$$R_{lum}(z) = \int \frac{k_\nu(z)}{1+\varepsilon\tilde{S}(z)}\left[S_\nu^+(z) + S_\nu^-(z)\right]\frac{\mathrm{d}\nu}{h\nu};$$

ε is the nonlinearity parameter; $r_{lum}(z)$ is the spectral power of spontaneous radiation emitted by the unit volume of the active layer at the point z of the resonator axis; a is a parameter determining the contribution of spontaneous radiation to amplified luminescence; n is the electron concentration; J is the pump current density; d is the active layer thickness; and A, B, and C are the coefficients of monomolecular, radiative (spontaneous), and Auger recombination, respectively. The parameter $b(z)$ is introduced due to the averaging of quantities $S_\nu^+(z)$ and $S_\nu^-(z)$ within some solid angle relative to the resonator axis z. This angle is mainly determined by total internal reflection from facets of the active medium. When the length L of the active layer greatly exceeds its thickness d and width w, the

L.I.Burov, I.N.Varaksa, A.G.Ryabtsev Belarussian State University, prosp. F.Skoriny 4, 220050 Minsk, Belarus;
S.V.Voitikov, M.I.Kramar, G.I.Ryabtsev B.I.Stepanov Institute of Physics, National Academy of Sciences of Belarus, prosp. F.Skoriny 68, 220072 Minsk, Belarus

Received 3 October 2001
Kvantovaya Elektronika **32** (3) 260 – 263 (2002)
Translated by M.N.Sapozhnikov

dependence of the parameter b on the coordinate z can be neglected, by assuming $b \approx 1$.

Note that radiation-transfer equations were earlier used to analyse the parameters of semiconductor lasers [2, 13–16]; however, the formation of laser radiation, taking amplified luminescence into account, was not studied in detail.

The solution of system of equations (1), (2) was found numerically in the quasi-stationary approximation using the iteration procedure. Material parameters were calculated for stripe $In_xGa_{1-x}As_yP_{1-y}/InP$ ILs emitting at 1.3 μm ($x = 0.72$, $y = 0.6$) and 1.55 μm ($x = 0.58$, $y = 0.9$) with bulk and quantum-well active layers. The thickness of the bulk active layer was 0.2 μm and the thickness of the quantum-well active layer was 80 Å. The spectral parameters $k_\nu(z)$ and $r_{\rm lum}(z)$ of the IL were calculated using models of parabolic zones both with and without the fulfilment of the selection rules for the wave vector. The reflection coefficients $r_1 = r_2$ of the mirror facets of a Fabry–Perot resonator were assumed equal to 0.32.

The IL characteristics were numerically simulated in the temperature range from 250 to 400 K using the Mathematics-4.0 computer algebra package. The temperature dependence T of the Auger recombination coefficient C (in $m^6 s^{-1}$) for the bulk active layer was described by the semiempirical expression [17]

$$C(T) = (28.8 \times 10^{-40}) E_{\rm g}^{-2} \exp\left(-\frac{0.12 E_{\rm g}}{kT}\right), \tag{3}$$

where $E_{\rm g}$ is the energy gap in electronvolts. This dependence for the quantum-well active layer was described by the expression [17]

$$C(T) = C_0 \exp\left(-\frac{E_{\rm a}}{kT}\right), \tag{4}$$

where $E_{\rm a}$ and C_0 are the activation energy and the normalisation constant, respectively. The values of $E_{\rm a}$ and C_0 were calculated by the interpolation of the Auger recombination coefficients at different temperatures [9]. The temperature dependences of the spontaneous recombination coefficient B for the bulk [19, 20] and quantum-well [10, 20] active layers were calculated using the relevant data from the literature. In particular, for the IL with a bulk active layer, the value of B varied from 8.34×10^{-17} to 4.20×10^{-17} $m^3 s^{-1}$ for $T = 200 - 400$ K.

The type of the temperature dependence $\rho(T)$ of the internal optical losses for the IL with the bulk active layer emitting at 1.55 μm was assumed the same as for the IL emitting at 1.3 μm [21]; however, the values of $\rho(T)$ for the IL emitting at 1.55 μm were taken from paper [19]. The dependence $\rho(T)$ (in reciprocal metres) for the quantum-well IL emitting at 1.55 μm was approximated by the expression [10]

$$\rho(T) = \exp(3.15 + 0.01T), \tag{5}$$

where T is in kelvins. The ratio of values of $\rho(T)$ at 1.3 and 1.55 μm for the quantum-well IL was assumed the same as for the IL with the bulk active layer. We also assumed that the monomolecular recombination coefficient A was 10^8 s^{-1} for all ILs and was independent of temperature. The parameter a in (1) was set equal to 0.4 according to the results [12] applied to the laser system under study. The initial values of the gain were taken from the calculated recombination rate [7, 8] and the nonlinearity parameter ε was assumed equal to 2.3×10^{-12} $m^2 W^{-1}$ [22].

We solved the system of equations (1), (2) by specifying the concentration n_0 of nonequilibrium carriers, which were uniformly distributed over the resonator length. This concentration corresponds to a certain injection current J for $n_0 > n_{\rm e}$, where $n_{\rm e}$ is the transparency concentration at which the gain is zero. The required parameters were calculated based on this concentration, and the system of equations (1), (2) for $S_\nu^{\pm}(z)$ was solved in the entire spectral range. Then, the integrated current density

$$S(z) = \int \left[S_\nu^+(z) + S_\nu^-(z)\right] d\nu,$$

was determined, which corresponds to the density of the amplified luminescence flux along the resonator axis. Then, we determined the spectral distribution of the gain taking into account the saturation effect, using $\tilde{S}(z)$ instead of $S(z)$ (the error upon such a substitution did not exceed 5×10^{-4} because the parameter ε is small), and found more exactly the distribution $n(z)$ of concentration of carriers along the resonator axis. The iteration procedure was repeated successively to obtain the required convergence. After iterations, the integrated density of amplified luminescence was defined as the function of the carrier concentration, i.e., $S(z) = S[n(z)]$.

The values of n and $R_{\rm lum}$ were successively calculated at different temperatures in the range from 250 to 400 K. Then, the threshold carrier concentrations $n_{\rm th}$ and the corresponding rates $R_{\rm lum}^{\rm th}$ were determined. The calculated dependences $R_{\rm lum}^{\rm th}(T)$ are shown in Fig. 1. One can see that the rate $R_{\rm lum}^{\rm th}$ of recombination induced by amplified luminescence at the lasing threshold increases in fact exponentially with temperature for all ILs studied. Weak deviations from the exponential dependence can be explained by the approximations used in calculations. It follows from Fig. 1 that the temperature dependence of the recombination rate $R_{\rm lum}^{\rm th}$ becomes stronger with increasing the lasing wavelength (cf. the dependences shown by solid

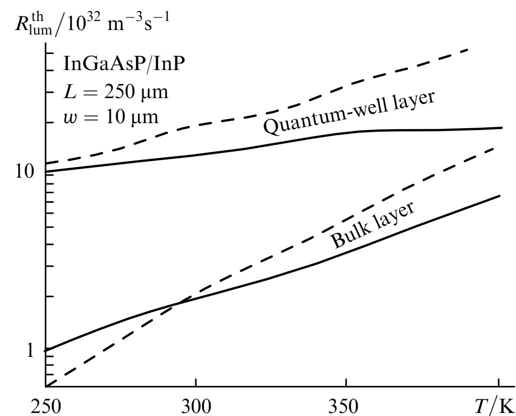

Figure 1. Temperature dependences of the recombination rate $R_{\rm lum}^{\rm th}$ induced by amplified luminescence at the lasing threshold of the injection InGaAsP/InP laser with bulk and quantum-well active layers emitting at 1.3 (solid curves) and 1.55 μm (dashed curves).

and dashed curves). This is explained by the increase in the gain and the width of the spectrum of the InGaAsP/InP IL with increasing the lasing wavelength.

The recombination rate $R_{\mathrm{lum}}^{\mathrm{th}}$ for the quantum-well IL (the upper curves in Fig. 1) is almost an order of magnitude greater than that for the IL with a bulk active region (the lower curves in Fig. 1). The difference somewhat decreases with increasing temperature, remaining, however, quite considerable. Such a relation between recombination rates can be explained by the fact that, as follows from calculations of the gain spectra, the ratio of the width of the spectrum to its maximum is much greater in the IL with the bulk active layer than in the quantum-well IL.

The threshold density J_{th} of the injection current at different temperatures can be found from the rate equations [6, 7]

$$J_{\mathrm{th}}(T) = ed\left[An_{\mathrm{th}}(T) + Bn_{\mathrm{th}}^2(T) + Cn_{\mathrm{th}}^3(T) + R_{\mathrm{lum}}^{\mathrm{th}}(T)\right]. \quad (6)$$

Fig. 2 shows the dependences $J_{\mathrm{th}}(T)$ calculated for the quantum-well IL and the IL with the bulk active layer. It follows from these dependences that recombination induced by amplified luminescence causes the increase in the threshold current for all the ILs under study in the entire temperature range. Table 1 presents the threshold current densities calculated taking into account the amplified luminescence (J_{th}) and neglecting it (J_{th}^-); also, the ratio $J_{\mathrm{th}}/J_{\mathrm{th}}^-$ at $T = 300$ K is presented for ILs under study.

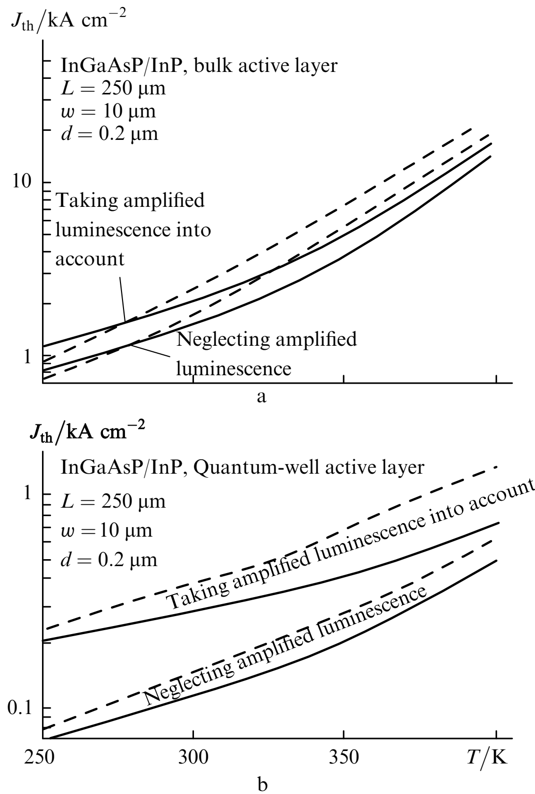

Figure 2. Temperature dependences of the threshold current density J_{th} for ILs with bulk (a) and quantum-well (b) active layers emitting at 1.3 μm (solid curves) and 1.55 μm (dashed curves) calculated taking the amplified luminescence into account or neglecting it.

Table 1. Comparative values of threshold current densities J_{th} and J_{th}^- at 300 K.

Active layer	λ/μm	J_{th}/kA cm^{-2}	J_{th}^-/kA cm^{-2}	$J_{\mathrm{th}}/J_{\mathrm{th}}^-$
Bulk	1.3	2.09	1.49	1.41
	1.55	2.39	1.74	1.37
Quantum-well	1.3	0.28	0.11	2.53
	1.55	0.39	0.15	2.65

One can see from Table 1 that the ratio $J_{\mathrm{th}}/J_{\mathrm{th}}^-$ for the quantum-well IL emitting at 1.55 μm is 2.65 at 300 K. This ratio decreases with increasing temperature, however, it remains at the level of 2.1 even at 400 K.

We also calculated the temperature dependences of the characteristic parameter T_0 ($J_{\mathrm{th}} \sim \exp(T/T_0)$) for quantum-well ILs and ILs with the bulk active layer (Fig. 3). One can see that the temperature dependence $T_0(T)$ agrees qualitatively with experimental data obtained for quantum-well ILs [23].

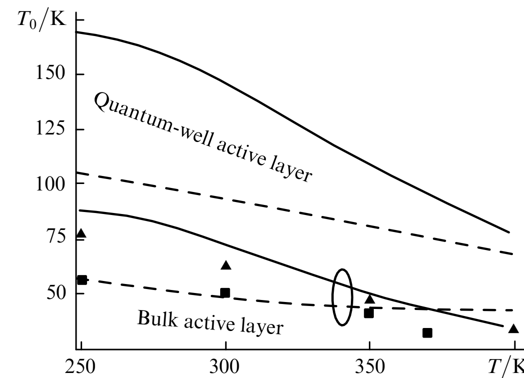

Figure 3. Temperature dependences of the parameter T_0 for ILs with quantum-well and bulk active layers emitting at 1.3 μm (solid curves and triangles) and 1.55 μm (dashed curves and squares). The experimental data were obtained for the quantum-well InGaAsP IL with the resonator length $L = 1$ mm and width $w = 2$ μm [23].

Thus, by solving radiation-transfer equations, we studied the effect of amplified luminescence on the lasing threshold of long-wavelength InGaAsP/InP lasers with bulk and quantum-well active layers emitting at 1.3 and 1.55 μm. This method allows us to take into account the geometry of the active layer in the analysis of threshold characteristics of the ILs. We have found that amplified luminescence can increase the threshold current density by a factor of two and more. This fact agrees with the results of paper [24].

The effect of amplified luminescence on the dependence $J_{\mathrm{th}}(T)$ is most pronounced in lasers emitting at longer wavelengths. All other factors being the same, the contribution of amplified luminescence to $J_{\mathrm{th}}(T)$ is greater for quantum-well ILs.

References

1. Basov N.G., Bogdankevich O.V., Pechenov A.N., Nasibov A.S., Fedoseev K.P. *Zh. Eksp. Teor. Fiz.*, **55**, 1710 (1968).
2. Bogdankevich O.V., Darznek S.A., Zverev M.M., Ushakhin V.A. *Kvantovaya Elektron.*, **2**, 1757 (1975) [*Sov. J. Quantum Electron.*, **5**, 953 (1975)].

3. Gribkovskii V.P., Kononenko V.K., Ryabtsev G.I., Samoilyukovich V.A. *IEEE J. Quantum Electron.*, **12**, 322 (1976).
4. Gribkovskii V.P. *Prog. Quantum Electron.*, **19**, 41 (1995).
5. Voronin V.F., Gribkovskii V.P., Inozemtsev K.I., Ryabtsev G.I., Samoilyukovich V.A., Yashumov I.V. *Zh. Prikl. Spektrosk.*, **37**, 386 (1982).
6. Voronin V.F., Gribkovskii V.P., Zhukov N.D., Ryabtsev G.I., Sosnovskii S.A. *Zh. Prikl. Spektrosk.*, **43**, 40 (1985).
7. Gribkovskii V.P., Voitikov S.V., Kramar M.I., Ryabtsev G.I., Kragler R. *Nonlinear Phenomena in Complex Systems*, **2**, 6 (1999).
8. Burov L.I., Kramar M.I., Kuleshov A.A., Ryabtsev G.I., Shore K.A., Voitikov S.V. *Symp. High Performance Electron Devices for Microwave & Optoelectronic Applications* (London, 1999) pp 278–283.
9. Duraev V.P., Ryabtsev G.I., in *Obzory po elektronnoi tekhnike. Ser. 11. Lazernaya tekhnika i optoelektronika* (Reviews on Electronic Devices. Ser. 11. Lasers and Optoelecronics) (Moscow: 'Electronika', Central Research Institute, 1988) No. 5 (1376) p. 48.
10. Zou Y., Osinski J.S., Grodzinski P., Dapkus P.D., Rideout W.C., Sharfin W.F., Schlafer J., Crawford F.D. *IEEE J. Quantum Electron.*, **29**, 1565 (1993).
11. Yoshida Y., Watanabe H., Shibata K., Takemoto A., Higuchi H. *IEEE J. Quantum Electron.*, **34**, 1257 (1998).
12. Samson A.M. *Zh. Prikl. Spektrosk.*, **2**, 232 (1965).
13. Sommers H.S., North D.O. *Solid-State Electron.*, **19**, 675 (1976).
14. Sommers H.S. *J. Appl. Phys.*, **53**, 156 (1982).
15. Yang W., Gopinath A. *Appl. Phys. Lett.*, **63**, 2717 (1993).
16. Tromborg B., Lassen H.E., Olesen H. *IEEE J. Quantum Electron.*, **30**, 939 (1994).
17. Frojdh K., Holmstrom P., Olin U. *Technical Report 'TR 310, 961120'* (Stockholm, Inst. of Optical Research, 1996, S-100 44).
18. O'Reilly E.P., Adams A.R. *IEEE J. Quant. Electron.*, **30**, 366 (1994).
19. Kakimoto S., Watanabe H. *IEEE J. Quant. Electron.*, **34**, 540 (1998).
20. Garbuzov D.Z., Agaev V.V., Sokolova Z.N., Khalfin V.B., Chalyi V.P. *Fiz. Tekh. Poluprovodn.*, **18**, 1069 (1984).
21. Voronin V.F., Gribkovskii V.P., Duraev V.P., Ryabtsev G.I. *Zh. Prikl. Spektrosk.*, **47**, 204 (1987).
22. Wang J., Griesinger U.A., Schweizer H. *Appl. Phys. Lett.*, **69**, 1585 (1996).
23. Phillips A.F., Sweeney S.J., Adams A.R., Thijs P.J.A. *IEEE Select. Topics in Quantum Electron.*, **5**, 401 (1999).
24. Chuang S.L., O'Gorman J., Levi A.F.J. *IEEE J. Quantum Electron.*, **29**, 1631 (1993).